Altimetry
Mesoscale
Variability
Oceanic
Review

Atimétrie
Mésoéchelle
Variabilité
Océanique
Revue

Contribution of satellite altimetry to the observation of oceanic mesoscale variability

Pierre-Yves LE TRAON

CLS Argos, 18, avenue Edouard Belin, 31055 Toulouse Cedex, France.

ABSTRACT

The long duration and low noise level offered by the US Navy's Geosat altimeter opened up new scope for the quantitative use of satellite altimetry in observing oceanic mesoscale variability. This paper, centered on recent results from Geosat data, shows how satellite altimetry contributes to the description of oceanic mesoscale variability. The methods commonly used to extract the oceanic mesoscale signal are first recalled. We briefly discuss their impact on the signal, and measurement errors. We then look at the results of comparisons between altimeter data and *in situ* measurements, and demonstrate that Geosat data are suitable for observing mesoscale variability. The unique contribution which altimetry can make comes from its global space-time coverage, which provides a quasi-synoptic description of the ocean circulation and a statistical description to an unrivalled degree of detail. A few examples illustrate the innovative contribution which synoptic mapping can provide. But the greatest contribution is in the statistical description of ocean mesoscale variability. We review several papers dealing with the global statistical description of mesoscale variability and its seasonal variations, characterization of space and time scales and frequency-wave number spectral analysis, and statistical descriptions of western boundary currents. All confirm the unique contribution which satellite altimetry can make to the statistical description of mesoscale phenomena.

Oceanologica Acta, 1992. **15**, 5, 441-457.

RÉSUMÉ

Apport de l'altimétrie à l'observation de la circulation mésoéchelle

En raison de son faible niveau de bruit et de sa longue durée de vie, le satellite altimétrique de l'US Navy Geosat a ouvert de nouvelles perspectives pour l'étude quantitative de la variabilité mésoéchelle océanique. Cet article traite principalement des résultats récents obtenus grâce à Geosat en essayant de mettre en avant les contributions originales de l'altimétrie pour l'étude de la variabilité océanique mésoéchelle. On rappelle les méthodes habituellement utilisées pour extraire le signal océanique mésoéchelle. L'impact de ces méthodes et les erreurs de mesure sont brièvement discutés. La capacité de Geosat pour l'observation de la variabilité mésoéchelle est ensuite démontrée en utilisant les résultats des comparaisons entre les données de Geosat et les mesures *in situ*. L'apport de l'altimétrie vient de sa couverture spatio-temporelle globale, qui permet une description quasi-synoptique de la circulation océanique et une description de type statistique avec un détail inégalable. A travers quelques exemples significatifs, l'apport nouveau lié à la possibilité de cartographie synoptique est montré. C'est dans la description statistique de la variabilité mésoéchelle océanique que l'apport est cependant le plus évident. De nombreux articles traitant de la description statistique globale de la variabilité mésoéchelle et de ses variations saisonnières, de la caractérisation des

échelles spatiales et temporelles et de l'analyse des spectres en fréquence et en nombre d'onde, et de la caractérisation statistique des courants de bord ouest sont revus. Ils montrent clairement la contribution unique de l'altimétrie satellitaire pour la description statisitique de la mésoéchelle.

Oceanologica Acta, 1992. **15**, 5, 441-457.

INTRODUCTION

It is now established that oceanic circulation varies over a wide range of space and time scales ranging from tens to thousands of kilometers and from days to years (*e. g.*, Wunsch, 1981). The term mesoscale or eddy variability usually refers to a sub-class of energetic motions with typical space and time scales of 50 to 500 km and 10 to 100 days. However, in practice it is often impractical to isolate longer time-scale fluctuations from mesoscale variability, so that the definition in this paper is rather broad. Phenomenological representations of this variability include eddies, fronts, meanders, rings and planetary waves. Over the past thirty years, a major effort has been made to observe and model eddy variability. Our understanding has progressed a lot and the eddy field has been visualized qualitatively (Robinson, 1982). Ocean eddies can be observed almost everywhere at mid and high latitudes, their energy generally exceeding the energy of the mean flow by an order of magnitude or more. They are forced by instability of the large-scale circulation, by wind fluctuations, by the scattering of currents off topography. From these source regions, eddy energy is redistributed throughout the oceanic gyre by complex processes which we do not yet completely understand. They lose energy to smaller scales by dissipation but can also feed energy back to the mean flow (Holland *et al.*, 1982). They also transport heat although their climatic role is not yet well established.

Despite all this progress, our understanding of eddy dynamics remains incomplete and mostly qualitative. In particular, much of our understanding comes from eddy-resolving numerical models, and we do not have enough oceanic evidence. We now need observations over larger areas and longer time spans. These will help, for example, to quantify the energy sources of eddies and their interaction with the general circulation, to rationalize their structures and to estimate their contribution to the total heat transport. In this respect, satellite altimetry has unique capabilities for producing a global and synoptic view of the oceans, even in remote areas. Satellite altimetry can accurately measure the variable part of the sea surface topography. Since mesoscale eddies are mainly in geostrophic equilibrium, this translates directly into velocity measurements. Spatial sampling along the satellite ground track is ideal for mesoscale studies while a temporal sampling period of ten-twenty days should avoid aliasing of most of the mesoscale signal. Extensive, global space-time sampling is a unique means of describing mesoscale phenomena. This description is, of course, limited to the surface oceanic circulation. However, given the high vertical coherence of mesoscale variability, this information reflects more than just surface conditions and, when assimilated in ocean models, is a strong constraint for inferring the three-dimensional oceanic mesoscale circulation.

Four satellites have carried altimeters for earth observations: Skylab (1973), Geos-3 (1975), Seasat (1978) and Geosat (1985-1989). Noise levels have decreased steadily: 60, 25, 5 and 3.5 cm for 1-s averages. The oceanographic results obtained with Skylab, Geos-3 and Seasat have been reviewed by Fu (1983 *a*). The US Navy's Geosat altimeter opened new horizons for the quantitative use of satellite altimetry. Because of its long duration - the satellite operated on a near-repeat orbit (17.05-day cycle) for almost three years (November 1986 through June 1989) - and its low noise level, Geosat is particularly suitable for mesoscale observations (Cheney *et al.*, 1986; Douglas and Cheney, 1990). This was also emphasized in two special issues of the *Journal of Geophysical Research* in 1991. We now know that satellite altimetry can make a major contribution to the observation of mesoscale variability.

Most of the discussion in this paper therefore centers on recent results obtained from Geosat data, and shows how satellite altimetry contributes to the description of oceanic mesoscale variability. The second section recalls the different methods for extracting the mesoscale signal from altimetry and discusses their impact on the signal. The comparison of Geosat data with *in situ* measurements is examined in the third section. The contribution of satellite altimetry to synoptic and statistical descriptions of mesoscale circulation is then examined, respectively. The last section provides the main conclusion.

EXTRACTION OF THE MESOSCALE VARIABILITY FROM ALTIMETRY

If we disregard measurement errors, the sea surface topography measured by an altimeter consists of the geoid and the dynamic topography related to oceanic currents. Present geoids are not generally accurate enough to estimate absolute dynamic topography, except at very long wavelengths (> 5 000 km) and where accurate gravimetric geoids are available. A dedicated gravimetric mission is needed to enhance our knowledge of the geoid. An alternative approach would be to estimate a "synthetic geoid" by combining *in situ* oceanographic measurements with altimeter data (*e. g.*, Mitchell *et al.*, 1990; Glenn *et al.*, 1991).

The variable part of the dynamic topography is, however, easily extracted since no prior knowledge of the geoid height is needed. The most commonly used method is the so-called repeat-track method [collinear analysis (*e. g.*,

Ménard, 1983)]. It is suitable for satellites whose orbits repeat their ground tracks (to within ± 1 km) at regular intervals. For a given track, the variable part of the signal is thus obtained by removing the mean profile which contains the geoid and the quasi-permanent dynamic topography from each profile. The crossover difference technique (*e. g.*, Fu *et al.*, 1987) does not require a repeating orbit since only differences at crossovers of the satellite tracks are analyzed. This makes the analysis more difficult and the spatial sampling is too coarse for mesoscale studies. A third method uses an altimetric mean sea surface as a reference (*e. g.*, De Mey and Ménard, 1989). It is the simplest but requires precise altimetric mean sea surfaces, particularly at short wavelengths, which are not yet available. However, it should be possible to obtain accurate estimations after the Topex-Poseidon and ERS-1 missions.

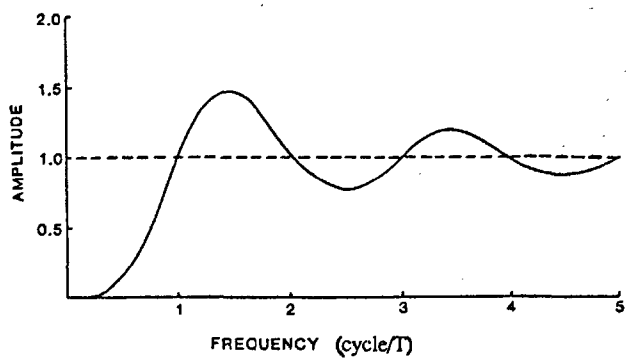

Figure 1

Transfer function of a filter for mean removal over time T (T = 24 days for Seasat, T = 2.5 years for Geosat) [adapted from Fu (1983 a)].

Fonction de transfert du retrait d'une moyenne sur une durée T (T = 24 jours pour Sesat, T = 2,5 années pour Geosat [adapté de Fu, 1983]).

Most scientists who have extracted mesoscale variability from Geosat data have used the repeat-track method. Figure 1, adapted from Fu (1983 *a*), shows how removing the mean impacts the temporal spectrum of mesoscale variability. The sampling rate also induces aliasing of frequencies higher than the Nyquist frequency (34 days^{-1} for Geosat). The variance of the error induced by removing the mean is typically $\langle h'^2 \rangle TI / T$ ($\langle h'^2 \rangle$ is variance of sea level variability, T is duration of observation and TI is decorrelation time of sea level variability). For Geosat, assuming decorrelation of one cycle in two (34 days), this amounts to a relative quadratic error of 10 % (30 % for the signal amplitude) for a one-year mean. Note also that this procedure is complicated by the fact that altimetric data are generally gappy. This means that only almost complete profiles can be used to estimate the mean profile (otherwise, there is contamination by the geoid signal as a result of orbit error). However, there are several ways of dealing with the problem (*e. g.*, Chelton *et al.*, 1990; Glenn *et al.*, 1991).

Altimeter measurements of sea surface topography are also affected by electromagnetic bias, inverse barometer effect, wet and dry tropospheric effects and ionospheric effects, ocean and terrestrial tides, residual geoid errors. As far as the mesoscale signal is concerned the more problematic corrections are wet tropospheric correction (if no radiometer on board) and inverse barometer effect. Note that for Geosat, SSM/I data provided an accurate estimation of the wet tropospheric correction after September 1987. Inverse barometer effect correction depends on the frequency-wave-number oceanic response to pressure forcing which is not well understood although encouraging progress has been made recently (*e. g.*, Ponte, 1992). However, numerous studies have shown that at mid-latitudes Geosat data are not over-contaminated by the effects mentioned above (*e. g.*, Fu, 1983 *b*; Bisagni, 1989; Jourdan *et al.*, 1990; Monaldo, 1990; Zlotnicki *et al.*, 1989; Le Traon *et al.*, 1990). Spectral analysis of these error sources shows, for example, that for wavelengths shorter than 1 000 km (mesoscale range), the oceanic signal is only slightly affected. The effect on geostrophic velocities is even smaller since the derivation reduces the effect of these long wavelength errors.

At this stage, the orbit error must still be corrected. The best orbits are currently accurate to within approximately 30 cm rms. However, since the orbit error is mainly long wavelength (one cycle per revolution, around 40,000 km), it can theoretically be separated from the mesoscale ocean signal which has characteristic spatial scales of a few hundred kilometres. This very long wavelength error is usually approximated by a first or second degree polynomial which is fitted to each altimeter profile. However, this polynomial adjustment method induces non-negligible errors on the mesoscale signal since there are not enough degrees of freedom to estimate the polynomial satisfactorily (Le Traon *et al.*, 1991). Figure 2 (reproduced from Le Traon *et al.*, 1991) illustrates the trade-off between having a long-arc and/or a low degree polynomial to minimize the errors

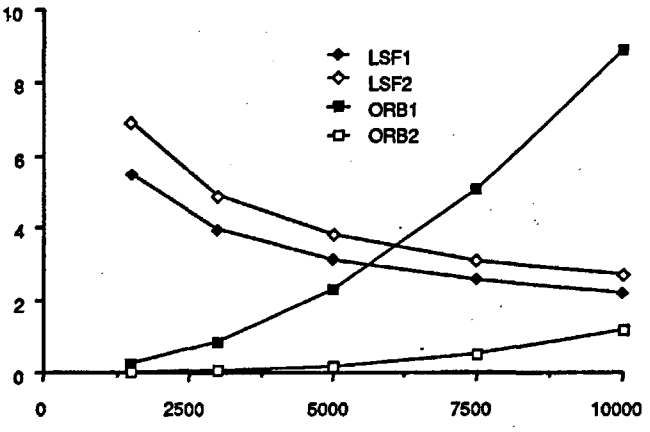

Figure 2

Rms errors in centimetres (averaged on the arc) due to first-degree (LSF1) and second-degree polynomial adjustments (LSF2) and corresponding orbit error modelling errors (ORB1 and ORB2) for different arc lengths (in kilometres). A homogeneous mesoscale signal of 15 cm rms and a 1-m rms orbit error are assumed (from Le Traon et al., *1991, reprinted by permission of the American Meteorological Society).*

Erreurs à un écart-type en centimètres (moyennées sur l'arc) dues à un ajustement par un polynôme de premier degré (LSF1) ou un polynôme de deuxième degré (LSF2), et erreurs de modélisation de l'erreur d'orbite correspondantes (ORB1 et ORB2) pour différentes longueurs d'arcs (en kilomètres). Le signal mésoéchelle de 15 cm (à un écart-type) est supposé homogène, et l'erreur d'orbite est de 1 m à un écart-type (d'après Le Traon *et al.*, 1991, reproduit avec la permission de l'American Meteorological Society).

induced by mesoscale variability and having a short-arc and/or high degree polynomial to minimize the effect of orbit error modelling error. For an orbit error of one meter rms and a mesoscale signal of 15 cm rms, it shows that, assuming an orbit error with a period of one cycle per revolution, a first degree polynomial fit on a 5 000 km long arc minimizes the sum of these two errors. The advantage of the polynomial fit is that it also removes some of the residual long-wavelength errors. Some authors have also tried to directly fit sine and cosine functions with periods of one cycle per revolution (*e. g.*, Chelton *et al.*, 1990). However, the orbit error spectra are more complex and these analyses may not remove all the orbit error. They also fail to remove residual long-wavelength errors. Note that the effect of the orbit error on geostrophic velocities is almost negligible (1 m orbit error at one cycle per revolution would induce an error on geostrophic velocities of about 1 cm s^{-1} at 45°N). The effects of polynomial fitting are also much smaller on geostrophic velocities. Through more complex methods using cross-track information, estimations of the orbit error can be considerably better constrained (*e. g.*, Tai and Fu, 1986; Tai, 1988). More generally using inverse techniques, the orbit error signal could be obtained through a global fit taking into account not only the spatial but also the temporal characteristics of the signal and noise (Blanc *et al.*, 1992). This should allow a better estimation of the mesoscale variability signal.

Hopefully most of the errors described in this section do not generally affect the mesoscale signal to any significant extent. Furthermore Geosat space-time sampling is well suited to mesoscale studies. This is confirmed in the next section.

VALIDATION AND COMPARISON WITH *IN SITU* DATA

Comparing altimetry with *in situ* measurements is not only useful for validation. It also highlights the different signals seen by the altimeter and *in situ* measurements, as well as the different space-time sampling modes. Any interpretation of the comparison must consider the different types of signals seen by various instruments. It is also important to consider the differences in space-time sampling characteristics and naturally the measurement errors. For example, dynamic heights obtained from hydrographic measurements (XBT, CTD) are not directly comparable with the altimetry: on their own, they provide only the baroclinic component of the signal while altimetry gives an absolute measurement of the variable signal (baroclinic and barotropic components). However, by choosing a deep enough level of no motion (*e. g.*, 1 000-2 000 dbar), the differences are only slight and the hydrographic measurements on their own can be compared with the altimetry. Another important point is that the altimetry provides only the variable part of the signal. And comparisons with velocity measurements (from current meters and drifters) must also take account of the fact that the altimetry provides only the geostrophic component of the surface current.

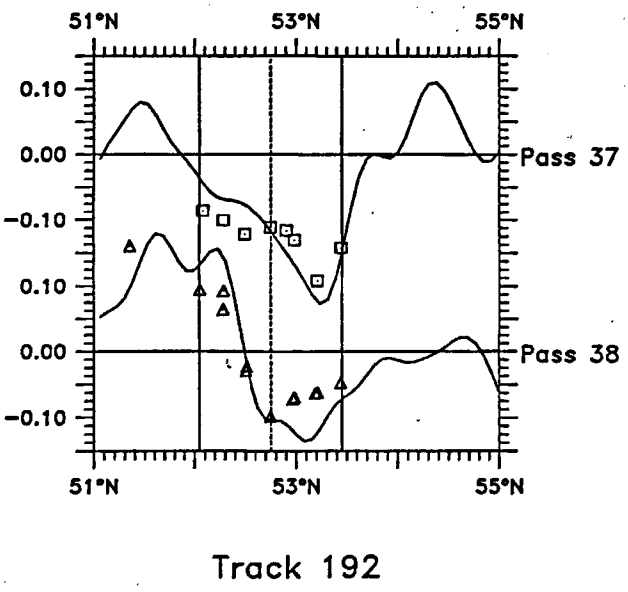

Figure 3

Comparison of Geosat dynamic topography anomaly (solid lines) and simultaneous dynamic topography anomaly obtained from XBT/CTD data for two consecutive cycles (squares and triangles) during the AthenA-88 experiment in the North-East Atlantic. A reference level at 1 000 dbar was assumed. Units are centimetres (from De Mey, 1992).

Comparaison de l'anomalie de la topographie dynamique déduite de Geosat (traits pleins) et de celle obtenue simultanément à partir de données XBT/CTD pour deux cycles consécutifs (carrés et triangles) pendant la campagne AthenA-88 dans l'Atlantique Nord-Est. Le niveau de référence a été fixé à 1 000 dbar. L'unité est le centimètre (d'après De Mey, 1992).

During the Athena-88 experiment in the North-East Atlantic, De Mey (1992) showed a good agreement between the along-track Geosat dynamic topography anomalies and dynamic height anomalies estimated from XBT/CTD with a 1 000-dbar reference level (*see* Fig. 3). Stammer *et al.* (1991) have compared Geosat measurements in the Iberian basin with dynamic height measurements referenced to 3000 dbar. Geosat data and hydrographic data were first objectively analyzed to obtain gridded values, and a climatological mean was added to Geosat maps to obtain absolute measurements of sea surface height. A high correlation (0.71) with hydrographic measurements was thus found with no significant bias despite the low signal-to-noise ratio of altimeter data in this part of the ocean (Fig. 4). Furthermore, the discrepancies are generally below the objective analysis mapping errors. As found by Willebrand *et al.* (1990; *see* below), the addition of a climatological mean to Geosat data improves the comparison very significantly.

Zlotnicki (pers. comm., 1991) has found good agreement between current-meter measurements and Geosat measurements in the Canary basin, despite a particularly weak velocity signal, on the order of 10 cm s^{-1}. Note, however, that the agreement was only obtained after suitable filtering of the current-meter data and Geosat data. Willebrand *et al.* (1990) have compared Geosat data with surface drifter data in the Gulf Stream extension area. Drifters were drogued at 100 m depth and were assumed to be good geostrophic cur-

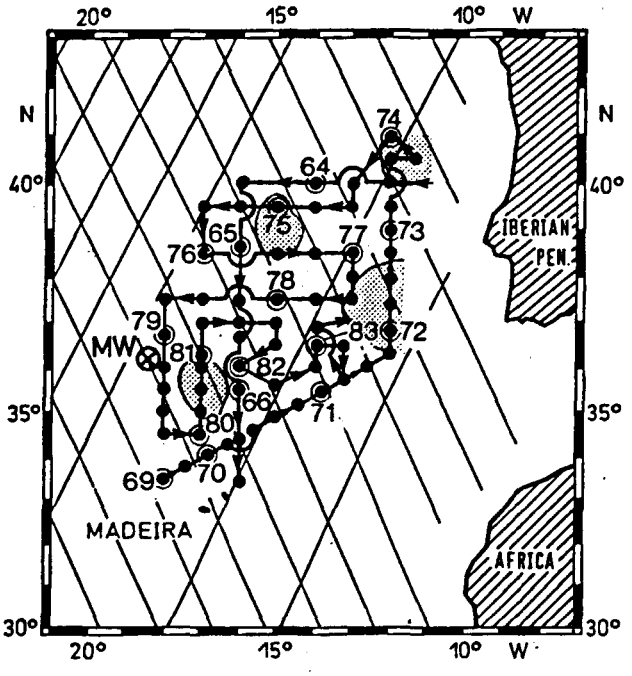

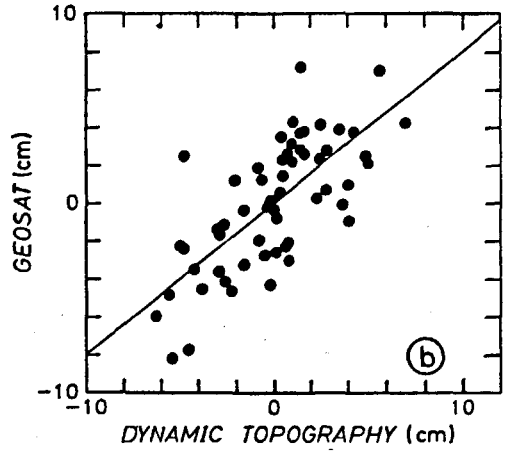

Figure 4

Comparison of Geosat data with hydrographic data in the Iberian basin. Geosat and hydrographic data (upper figure) were objectively analyzed and compared. The lower figure shows the scatter diagram of Geosat sea surface heights against dynamic topography 50/3000 dbar. A climatology is added to Geosat data for the comparison. The slope of the regression is 0.8 ± 0.2 and the correlation coefficient is equal to 0.71 [from Stammer et al., *1991 (copyright by the American Geophysical Union)].*

Comparaison des données de Geosat avec des données hydrographiques dans le bassin ibérien. Les données de Geosat et les données hydrographiques (figure du haut) ont été objectivement analysées et comparées. La figure du bas montre le diagramme de dispersion des hauteurs de surface de la mer mesurées par Geosat en fonction de la topographie dynamique 50/3000 dbar. Une climatologie a été ajoutée aux données de Geosat pour la comparaison. La pente de la régression est de 0,8 ± 0,2, et le coefficient de régression est égal à 0,71 [d'après Stammer *et al.*, 1991 (copyright par l'American Geophysical Union)].

rent followers. Sea surface height anomaly maps were constructed using an objective analysis procedure. Data over one cycle (seventeen days) were treated as synoptic. A mean dynamic topography was added to these maps to obtain an estimation of the absolute signal. Although the climatological field is very smooth and does not correspond to the mean field over the duration of the Geosat data set used in this study (fourteen months), it significantly improves the comparison with surface drifter data. The drifter trajectories agree well with these composite maps although a detailed comparison shows differences. The variance of the geostrophic velocity field deduced from Geosat maps is about a third of the variance of surface drifter velocities. However, this is the result of the objective analysis procedure. The variances before objective analysis agree very well, a result also found by Le Traon *et al.* (1990). In order to make comparisons, drifter data were objectively analyzed to estimate a streamfunction. The correlation between drifter velocities after objective analysis and Geosat geostrophic velocities is 0.81, with no significant bias. Note that the differences also reflect different mapping errors between Geosat and drifter data. Comparison between the dynamic topography at 50 dbar relative to 1 500 dbar along hydrographic sections also yielded general agreement except in regions of high mean gradients. This study validates Geosat data, most of the discrepancies being due to mapping errors related to coarse altimetric sampling. It also shows how useful it is to combine drifter and altimetry data (*see* also Le Traon and Hernandez, 1992). Also note the agreement in the Gulf Stream region between Geosat and the Doppler current-meter (ADCP) measurements (Joyce *et al.*, 1990) and inverted echo sounders with pressure gauges (IES/PGs; Hallock *et al.*, 1989).

Comparisons with AVHRR images have also validated the altimeter signal, even if, once again, the signals seen are not directly comparable (Vasquez *et al.*, 1990; Kelly and Gille, 1990). However, some eddies have very marked thermal structures, which can be used for qualitative comparisons providing that this signal is not masked by a surface signal from the mixed layer, as is usually the case during summer and fall.

Statistical comparisons have also been made. Le Traon *et al.* (1990) have compared Eddy Kinetic Energy (EKE) deduced from a set of historical drifter data with that deduced from Geosat data in the North Atlantic (Fig. 5). The agreement is very good and the mean ratio $\langle EKE_{buoys}/EKE_{Geosat}\rangle$ is about 1 with a standard deviation of 0.4. This also confirms that EKE as measured by drifters is essentially due to geostrophic currents, and that Geosat's temporal sampling is such that it can observe a large portion of the mesoscale variability. Le Traon *et al.* (1990) and Le Traon (1991) have also shown that the mesoscale spatial and temporal scales seen by Geosat are compatible with existing *in situ* measurements (CTD, currentmeters).

All these comparisons between Geosat altimeter data and *in situ* measurements confirm Geosat's capabilities for observing mesoscale circulation even in low eddy energy areas. This is an important and interesting result in itself. However, as mentioned earlier, the altimeter signals and *in*

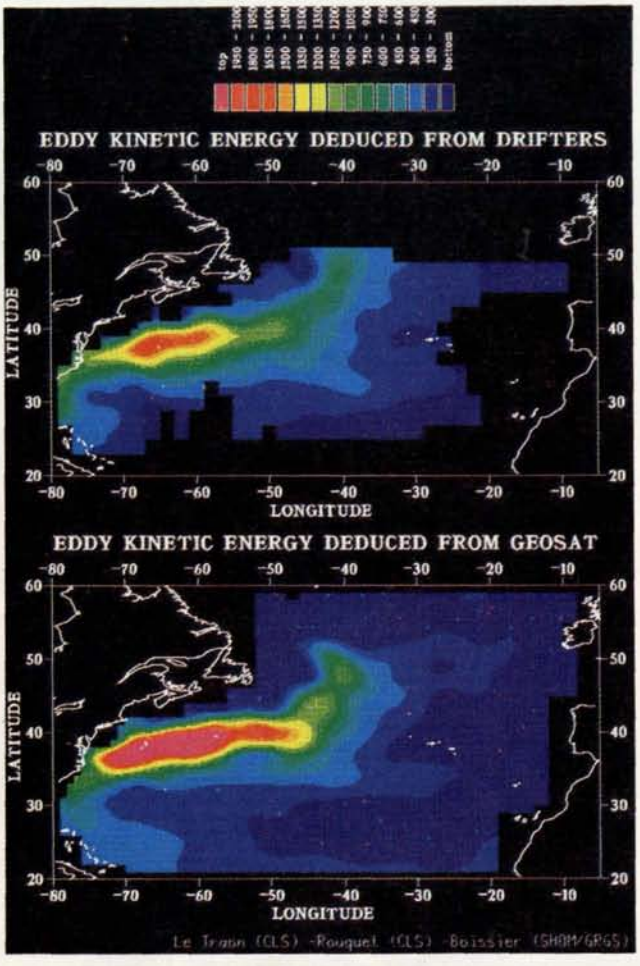

Figure 5

Eddy kinetic energy deduced from drifter data (upper figure) and from two years of Geosat data (bottom figure). The two maps show very good agreement. Note the high eddy kinetic energy in the Gulf Stream and in the North Atlantic drift and the low values in the eastern part of the basin [from Le Traon et al., *1990 (copyright by the American Geophysical Union)].*

Énergie cinétique tourbillonnaire obtenue à partir de données de flotteurs de surface (figure du haut) et de deux années de données de Geosat (figure du bas). Les deux cartes montrent un très bon accord. On peut noter les fortes valeurs d'énergie cinétique tourbillonnaire dans le Gulf Stream et dans la dérive nord-atlantique, et les faibles valeurs dans la partie est du bassin [d'après Le Traon *et al.*, 1990 (copyright par l'American Geophysical Union)].

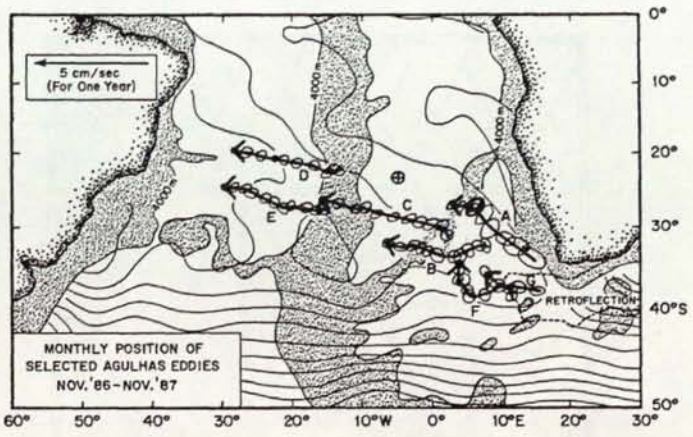

Figure 6

Trajectories of seven selected eddies which were followed using Geosat data. These are shown to be shed from the Agulhas retroflection into the South Atlantic subtropical gyre. Eddy positions and approximate size are shown as open symbols at roughly one month intervals [from Gordon and Haxby, 1990 (copyright by the American Geophysical Union)].

Trajectoires de sept tourbillons qui ont été suivis en utilisant les données de Geosat. On montre qu'ils se détachent de la rétroflection du courant des Aiguilles vers le gyre subtropical de l'Atlantique Sud. Les positions des tourbillons et leurs tailles approximatives sont données à des intervalles d'environ un mois, et sont représentées par des cercles [d'après Gordon et Haxby, 1990 (copyright par l'American Geophysical Union)].

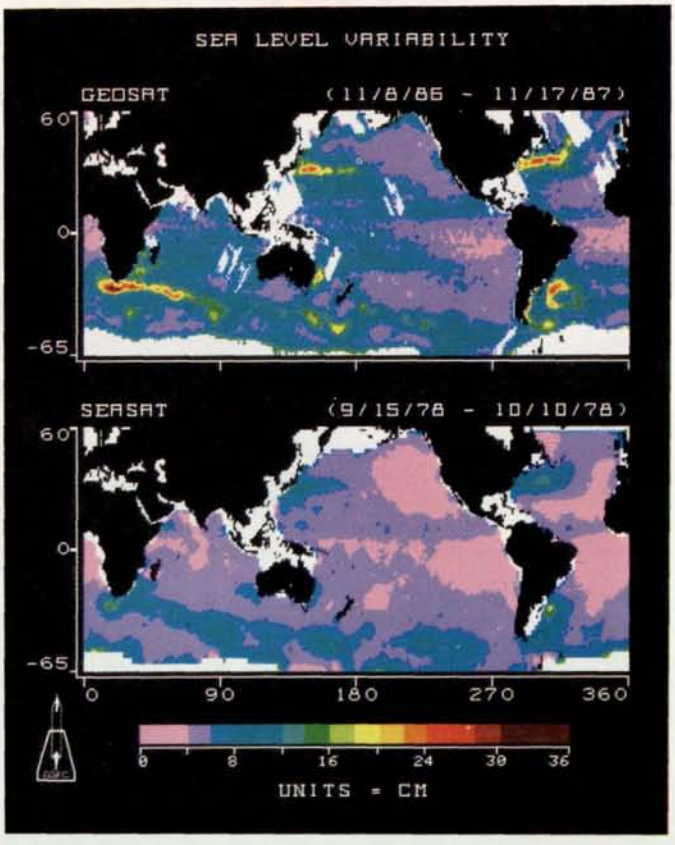

Figure 7

Rms sea level variability (in centimetres). Geosat versus *Seasat. The high variability in the area of western boundary currents (Gulf Stream, Kuroshio, Falkland, Algulhas) and the Antarctic Circumpolar Current (ACC) appears more clearly on the Geosat map (upper figure) since one month of Seasat data revealed roughly one third of the total rms signal [from Koblinsky, 1988 (copyright by the American Geophysical Union)].*

Écart-type de la variabilité du niveau de la mer (en centimètres). Geosat *versus* Seasat. Les fortes variabilités dans les régions des courants de bord ouest (Gulf Stream, Kuroshio, Falkland, Aiguilles) et le Courant Circumpolaire Antarctique (CCA) apparaissent plus clairement sur la carte de Geosat (figure du haut), puisqu'avec un mois de données, Seasat n'a pu observer qu'environ un tiers de l'écart-type du signal total [d'après Koblinsky, 1988 (copyright par l'Americain Geophysical Union)].

Figure 8

Rms variability of sea surface slope from one year of Geosat data. Units are μrad (3 μrad at 45°N corresponds to rms velocity of about 30 cms^{-1}). The contour marks 3 km ocean depth. Maximum variability can be observed again in western boundary currents and in the ACC. Note also the correlation between variability and ocean depth [from Sandwell and Zhang, 1989 (copyright by the American Geophysical Union)].

Écart-type de la variabilité de la pente à partir d'une année de données de Geosat. Les unités sont en μrad (3 μrad à 45°N correspondent à une vitesse de 30 cms^{-1}). Le contour représente la profondeur de 3 km. Les plus fortes variabilités sont de nouveau observées dans les courants de bord ouest et le CCA. On peut noter la forte corrélation entre la variabilité et la profondeur de l'océan [d'après Sandwell et Zhang, 1989 (copyright par l'American Geophysical Union)].

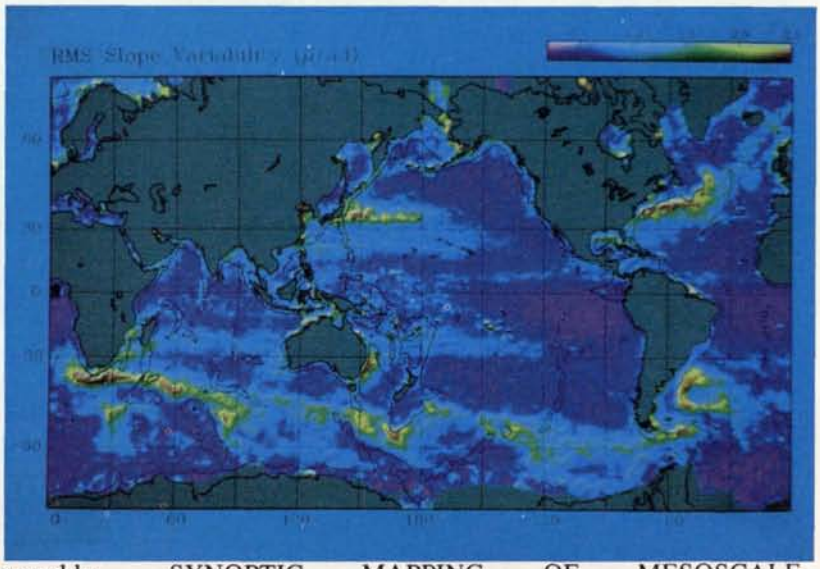

situ measurements are not generally directly comparable. The sampling modes are also different and the measurements are rarely simultaneous. This means that the absolute errors on the altimeter signal cannot be quantified precisely. This would call for dedicated calibration and validation experiments, as will be done for Topex-Poseidon. The effects of space-time sampling and analysis methods on the mapping of the complete signal must also be rationalized. This can be done *via* regional validation experiments such as, for example, Semaphore-93 (Eymard *et al.*, 1991).

SYNOPTIC MAPPING OF MESOSCALE VARIABILITY BY ALTIMETRY

Given its space-time sampling, satellite altimetry can provide synoptic mapping of mesoscale eddies. The accuracy of the mapping will depend, of course, on the orbit repeat period, and eddies at the center of the altimeter data grid may not be well resolved. Accurate mapping would require two simultaneous altimeter satellites, such as Topex-Poseidon and ERS-1. The mesoscale signal can then be

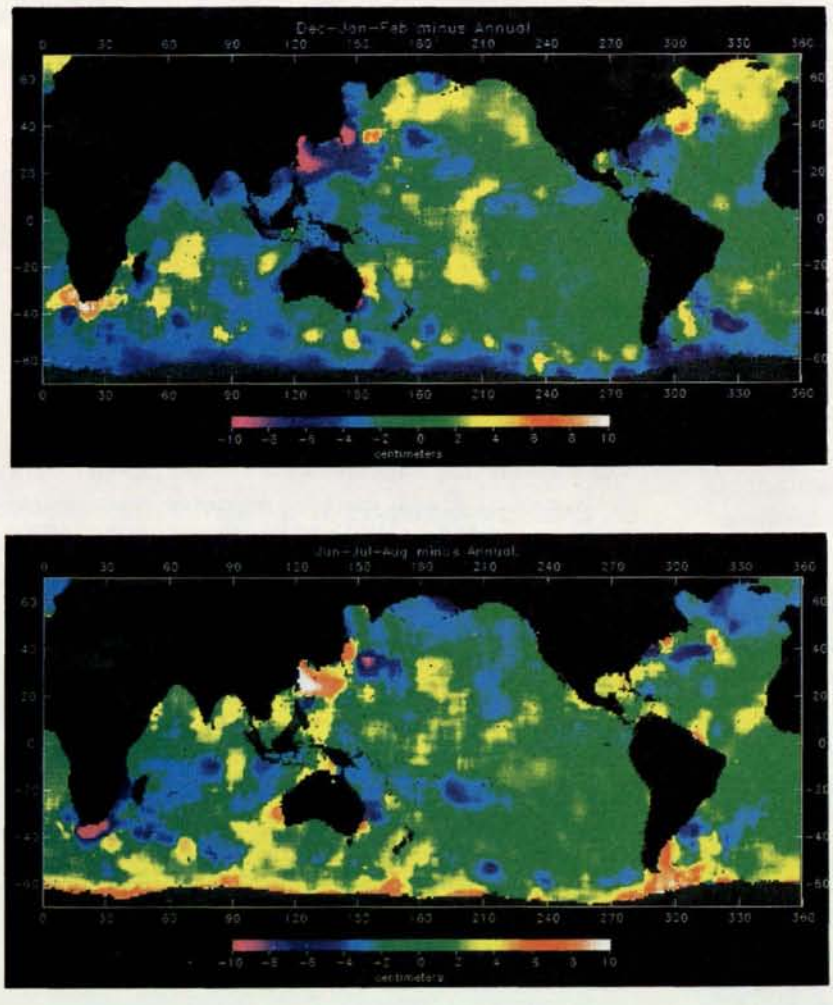

Figure 9

Rms sea level variability in centimetres for the winter season in the northern (upper figure) and southern (bottom figure) hemisphere (differences relative to the annual mean). North-East Pacific and North-East Atlantic show significant higher energy in the winter season, suggesting possible wind forcing (from Fu et al., *1988).*

Écart-type de la variabilité du niveau de la mer en centimètres pour la saison d'hiver de l'hémisphère Nord (figure du haut) et de l'hémisphère Sud [figure du bas (différences par rapport à la moyenne annuelle)]. Le Pacifique Nord-Est et l'Atlantique Nord-Est montrent des énergies significativement plus importantes pendant l'hiver, suggérant un forçage possible par le vent (d'après Fu *et al.*, 1988).

mapped very accurately (*e. g.*, Le Traon and Hernandez, 1992). However, the inter-track distance for Geosat is 1.475° which at mid-latitudes is generally less than the eddy spatial decorrelation scale. This means that the overall accuracy is acceptable even at the center of the altimeter data grid. The synoptic mapping capability of altimetry has been used by many investigators (*e. g.*, De Mey and Ménard, 1989; Fu and Zlotnicki, 1989; Gordon and Haxby, 1990; White *et al.*, 1990; Stammer *et al.*, 1991). By visualizing the eddies, their size, movement and deformation can be studied. This has made a significant contribution to our understanding of eddy dynamics.

Gordon and Haxby (1990) have analyzed a year of Geosat data in the Agulhas retroflection area of the Indian Ocean and the South Atlantic. Synoptic mapping of the mesoscale circulation at seventeen-day intervals over such a large area has revealed that anticyclonic eddies shed from the Agulhas retroflection migrate into the South Atlantic subtropical gyre at a rate of about five eddies a year (Fig. 6). They propagate westward at about 5 cm s^{-1} and need 2.5 years to cross the ocean. Gordon and Haxby (1990) infer that these eddies transport a sizeable 10 to 15 Sv of Indian ocean water (and salt and heat) into the South Atlantic. This result demonstrates the contribution which satellite altimetry can make. Clearly, a hydrographic section at a given time may not see these eddies and could miss their contribution. Global monitoring, as provided by satellite altimetry, is required.

Stammer *et al.* (1991) have used two years of Geosat data to map the eddy fields in the Iberian basin (30°-45°N to 20°W-10°W). By comparing Geosat data with hydrographic data (*see* the preceeding section), they have shown that the surface signature of mid-depth Mediterranean water lenses or meddies can be detected in Geosat sea surface height maps. They were also able to follow some meddies and estimated a 1.9 cm s^{-1} westward displacement, consistent with current knowledge of meddy movements. This is an interesting result because these signals are really weak. It also opens up new scope for the investigation of meddies with satellite altimetry.

White *et al.* (1990) have also objectively analyzed Geosat data over one year to track eddies in the California current region. This analysis has shown the wavelike structure of eddies and their westward propagation which has been further statistically analyzed (*see* the next section).

These studies clearly demonstrate that Geosat altimetry is capable of observing and monitoring the instantaneous ocean eddy field. As explained above, this helps to understand eddy dynamics better. It is also important for altimeter data assimilation. It shows that Geosat data can actually be assimilated into numerical oceanic models to infer the ocean three-dimensional circulation and its dynamics.

STATISTICAL DESCRIPTION OF MESOSCALE VARIABILITY BY ALTIMETRY

The global space-time sampling of satellite altimetry is a unique means of statistically describing mesoscale phenomena. Such a description can reveal differences between ocean regions and provide a global description of geographical and temporal (*e. g.*, seasonal) variation in mesoscale eddy statistics. This information can be used to rationalize their structure, identify sources of eddy energy, and analyze energy transfer from these sources. This will help us to understand eddy dynamics, particularly the mechanisms which generate and dissipate eddies. Global statistical descriptions are also a means of testing and validating models and are necessary for inverse modelling and altimeter data assimilation studies.

Global statistical description

The simplest description of mesoscale variability is that obtained by global mapping of either rms variability of the dynamic surface topography or of the variance of geostrophic velocity or slopes (*e. g.*, Koblinsky, 1988; Sandwell and Zhang, 1989; Shum *et al.*, 1990). These maps, generated from a year or more of Geosat measurements, essentially contain the mesoscale portion of the ocean signal but also any longer-period variations such as seasonal variations. Geosat has given us accurate global maps of these quantities. Koblinsky (1988) has compared the rms variability of the surface topography obtained by Seasat and Geosat (Fig. 7). With less than a month of measurements, Seasat revealed only a small part of the mesoscale spectrum, roughly a tenth of the total energy (*see* Fig. 1). The high variability in the area of western boundary currents (Gulf Stream, Kuroshio, Falkland, Algulhas) and the Antarctic Circumpolar Current (ACC) appears more clearly on the Geosat map, with maximum variability greater than 30 cm rms. Outside these areas, the signal is generally less than 8 cm rms. Sandwell and Zhang (1989) have produced a global map of the variance of dynamic topography slope, which translates directly into variance of geostrophic velocity outside equatorial areas (Fig. 8). They have established a correlation between the intensity of the variability and the ocean depth: areas of highest variability are in deep basins (> 4 km; *see* Fig. 8). Most of these areas are also characterized by intense mean currents (western boundary currents and ACC) which are the main source of eddy energy through instability. Fu *et al.* (1988) and Zlotnicki *et al.* (1989) have investigated the seasonal variations in eddy energy intensity (Fig. 9). These could be related to differences in wind forcing intensities which are higher during winter. Fluctuating wind forcing is thought indeed to be a possible source of eddy energy in regions far from western boundary currents (*e. g.*, Frankignoul and Müller, 1979; Müller and Frankignoul, 1981). Zlotnicki *et al.* (1989) have made a detailed analysis of these variations. After careful analysis of the different sources of errors, they concluded that some regions (North-East Atlantic and North-East Pacific) do show higher energy during winter. This suggests that wind forcing may be a source of eddy energy there. Shum *et al.* (1990) have done a global mapping of the geostrophic velocity variance and of its seasonal variations, which, assuming isotropy, is equal to the Eddy Kinetic Energy. More than 65 % of the ocean is shown to have EKE values less than 300 cm^2s^{-2}. The maximum EKE exceeds 2000 cm^2s^{-2} for most of the western boundary currents but reaches only 500 cm^2s^{-2} in the ACC. Significant seasonal variations were found in the Gulf Stream and

Kuroshio currents. The ACC system exhibits no apparent seasonal variation. Chelton *et al.* (1990) have undertaken a global investigation of the surface circulation of the Southern Ocean (south of 35°S) using two years of Geosat data. The altimeter data were carefully analyzed to estimate the mean profile and to remove the orbit error. Residual data were then averaged over 2° by 2° boxes to investigate the spatial and temporal variability of mesoscale variability.

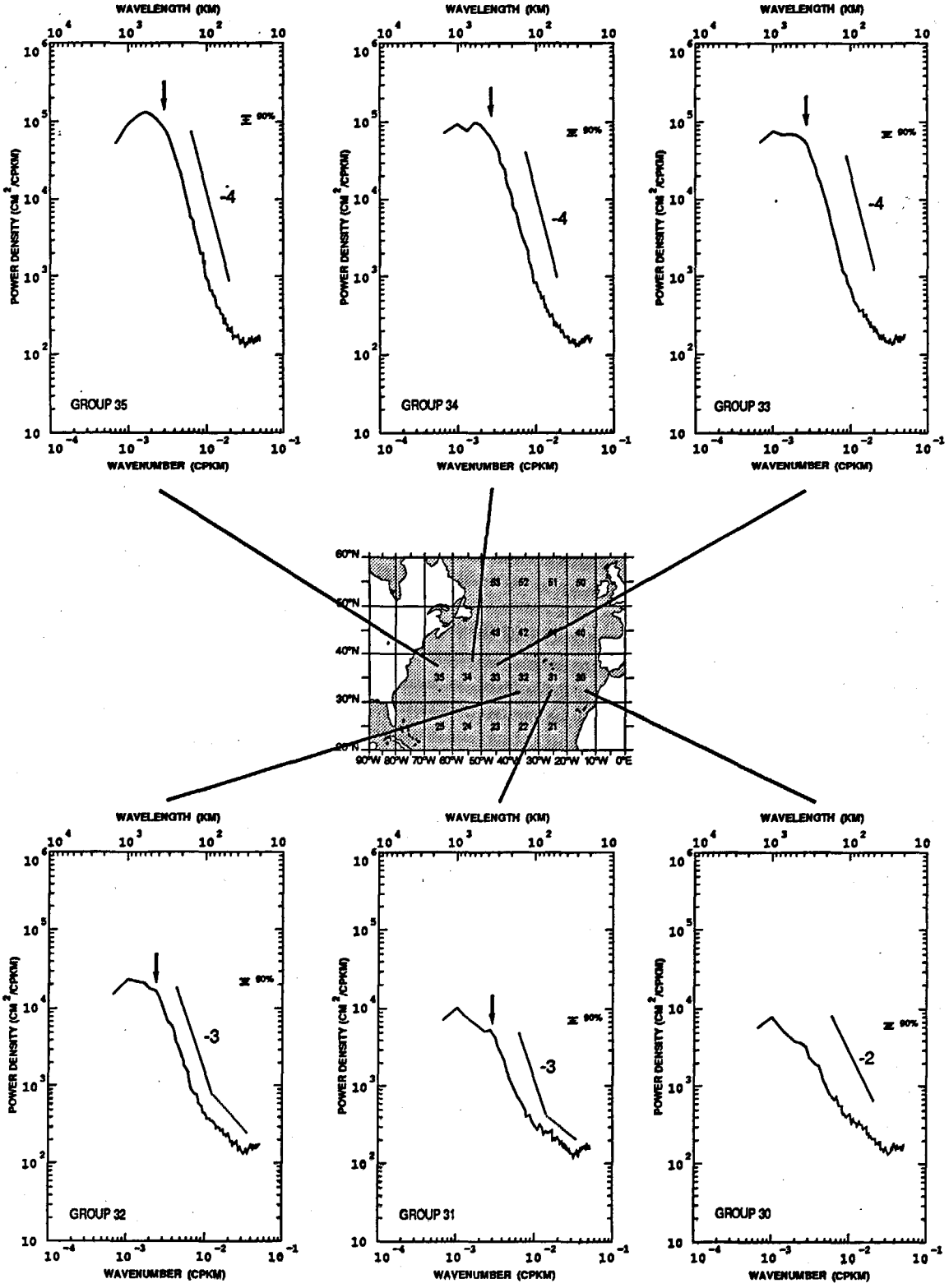

Figure 10

Mean wave number spectra of sea level variability in the North Atlantic on 10° in longitude by 10° in latitude areas deduced from two years of Geosat data. Breaks in spectral slopes are indicated by arrows [Le Traon et al., *1990 (copyright by the American Geophysical Union)].*

Spectres moyens en nombre d'onde dans l'Atlantique Nord sur des zones de 10° en longitude par 10° en latitude, obtenus à partir de deux années de données de Geosat. Les ruptures des pentes spectrales sont indiquées par des flèches [d'après Le Traon *et al.*, 1990 (copyright par l'American Geophysical Union)].

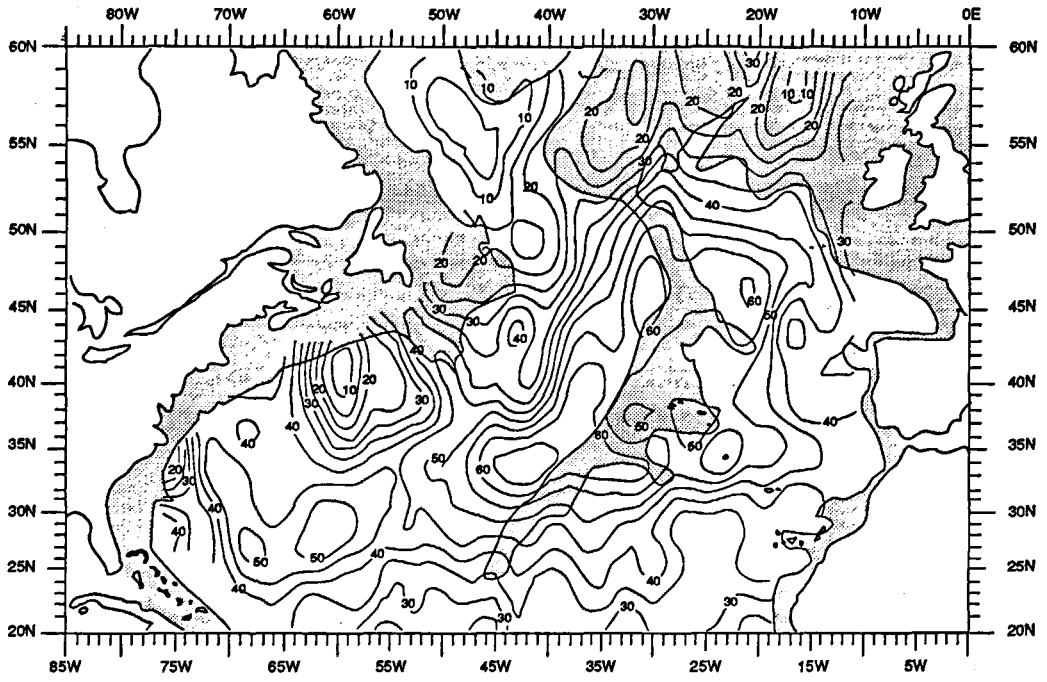

Figure 11

Seventeen-day isocorrelation map (x 100) of altimetric sea level variability in the North Atlantic deduced from two years of Geosat data. Depths shallower than 3 000 m are shaded. Time scales are shortest in areas of high mesoscale activity and/or strong mean currents (i. e. Gulf Stream and North Atlantic current), while relatively long time scales are found above the mid-Atlantic ridge and in the eastern part of the basin (Le Traon, 1991).

Isocorrélation à 17 jours (x 100) de la variabilité altimétrique du niveau de la mer dans l'Atlantique Nord obtenue à partir de deux années de données de Geosat. Les régions moins profondes que 3 000 m sont grisées. Les échelles temporelles sont les plus courtes dans les zones de forte activité mésoéchelle et/ou de forts courants moyens (*i. e.* Gulf Stream et dérive nord-atlantique), tandis que des échelles temporelles relativement grandes sont observées au-dessus de la dorsale médio-atlantique et dans la partie est du bassin (d'après Le Traon, 1991).

The results show a close relationship between the geographical distribution of mesoscale variability and the strength of the mean circulation of the ACC and Agulhas return current. This is not surprising since these narrow currents are likely to be baroclinically unstable. There is also strong topographic control of the eddy field (and the mean field) consistent with recent numerical simulation (*e. g.*, Treguier and Mc Williams, 1990). As also noted by Shum *et al.* (1990), there is surprisingly little seasonal or interannual variability in the eddy energy, in contrast with other major currents of the world ocean (*e. g.*, Gulf Stream, Kuroshio).

These descriptions have produced global, quantitative estimates of eddy energy with high spatial resolution. Spatial details have been revealed, such as the correlation with ocean depth and/or the mean currents. Geosat data have also provided, for the first time, a global description of the seasonal variations in eddy energy.

Characterization of space and time scales of mesoscale variability and spectral analysis

Le Traon *et al.* (1990) have produced a global statistical description of mesoscale variability in the North Atlantic using Geosat data. They have conducted a systematic study of wave-number spectra and have characterized the space scales of mesoscale variability. Their results provide a good match with *in situ* data and compare qualitatively with quasi-geostrophic turbulence models (Rhines, 1977; Hua and Haidvogel, 1986). Wave-number spectra are thus consistent with eddy forcing by instability of a mean current in the western side of the basin and with fluctuating wind forcing on the eastern side. Altimetric spectral slopes, however, are weaker, possibly due to non-geostrophic effects related to the mixed layer mesoscale variability. They are typically - 4 in the western part of the basin and between - 2 and - 3 in the other areas between 50-200 km and 200-600 km (Fig. 10). After the break in the slope, spectra remain red in the eastern part of the basin. Space scales typically decrease from west to east and south to north. Simple proportionality with respect to the first internal Rossby radii does not apply everywhere. This study has been complemented by a global description of time scales and their relationships with space scales in the North Atlantic by Le Traon (1991). Time scales are shortest in areas of high mesoscale activity and/or strong mean currents (*i. e.*, Gulf Stream and North Atlantic current), while relatively long time scales are found above the mid-Atlantic ridge and in the eastern part of the basin (Fig. 11). Bottom topography appears to play an important role in the temporal coherence of mesoscale structures. In general, time scales are not proportional to space scales. Frequency-wavenumber spectral analysis shows that the dominant wavelengths of around 200 to 600 km (depending on latitude) are associated with long periods (> 150 days) in the eastern part of the basin, while near the Gulf Stream significant energy is also found at shorter periods (Fig. 12). In the Gulf Stream area, propagation velocities are either westward or eastward for short periods (< 80 days). At longer periods and in the North-East Atlantic, they are mainly westward. Quasi-seasonal signals associated with westward propagations are also observed in these frequency-wave-number spectra (Le Traon, 1991). These results confirm the interpretation of wave-number spectra by Le Traon *et al.* (1990) who suspected a change in dynamic regime after the spectral wave-number peak. Indeed,

pseudo-dispersion relations deduced from Geosat data point to two distinct dynamic regimes, as in numerical models: a turbulent regime for smaller scales (< 300 to 500 km), where there is proportionality between space and time scales, and an apparently more linear regime after the spectral peak in wave number where an inverse dispersion relation is found in the eastern part of the basin. This latter feature is in agreement with quasi-geostrophic models forced by fluctuating winds (Treguier and Hua, 1987).

White *et al.* (1990) have done a statistical analysis of one year of Geosat data in the California Current region from 20° to 50°N, westward to 140°W. Complex empirical orthogonal function (CEOF) analysis reveals that 53 % of the signal variance is associated with the annual cycle, reaching a maximum in summer and a minimum in winter. The spatial phase distribution shows annual waves originating at the coast and propagating westward over 1-2 cycles. Zonal wave number-frequency analysis points to dominant wavelengths of 500-1 000 km with periods of 4-12 months and westward propagations. These results agree with recent results obtained with wind-forced models (Pares-Sierra *et al.*, 1992). At all latitudes, peaks in these spectra lay near the linear baroclinic Rossby wave dispersion curve. Park (1990) has also used frequency and wave number spectral analysis to reveal semi-annual baroclinic Rossby waves modified by the topography in the Crozet basin area of the ACC.

These frequency/wave number spectral characterizations (and the corresponding characterizations of time and space scales) are a new and unique contribution from satellite altimetry. They are very difficult to obtain from *in situ* measurements. Eddy statistics have been visualized in greater detail, often bringing new information. They should now be compared with the results of modelling. The comparison with models should also help us to better understand the observed frequency/wave number oceanic response and possibly relate it to the different kinds of forcing. Note that altimeter data have already been compared with models (*e. g.*, Pares-Sierra *et al.*, 1992; Stammer and

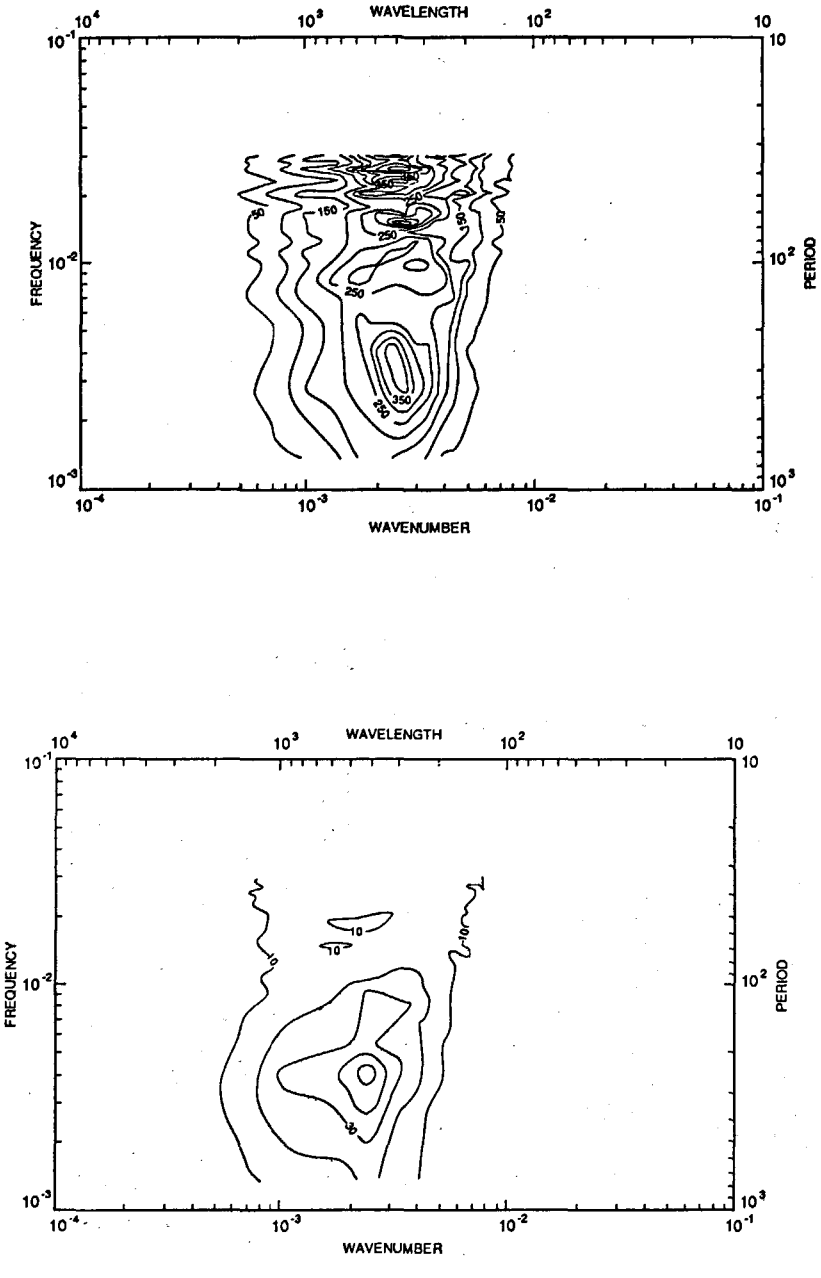

Figure 12

Mean frequency-wave number spectrum for the Gulf Stream area (30°N-40°N; 70°W-50°W). Units are square centimetres. Contour interval is 50 cm² (upper figure). Mean frequency-wavenumber spectrum for the Azores current area (30°N-40°N; 40°W-20°W). Contour interval is 10 cm² (bottom figure). The mean spectrum for the Gulf Stream area shows that the energy corresponds mainly to wavelengths between 200 and 600 km over a broad range of periods while the mean spectrum for the Azores current area shows very weak energy for periods shorter than 80 days. Note also that seasonal signals are observed in both spectra (Le Traon, 1991).

Spectre en fréquence et en nombre d'onde moyen pour la région du Gulf Stream (30°-40° N ; 70°-50° W). L'unité est le centimètre carré. L'intervalle de contour est de 50 cm² (figure du haut). Spectre en fréquence et en nombre d'onde moyen pour la région du courant des Açores (30°-40° N ; 40°-20° W). L'intervalle de contour est de 10 cm² (figure du bas). Le spectre moyen pour la région du Gulf Stream montre que l'énergie correspond principalement à des longueurs d'ondes comprises entre 200 et 600 km, et à une large gamme de périodes, tandis que le spectre moyen pour la région du courant des Açores montre très peu d'énergie pour les périodes inférieures à 80 jours (d'après Le Traon, 1991).

Böning, 1992; Tréguier, 1992). These comparisons must be continued and developed.

Statistical description of Gulf Stream and Kuroshio

Many studies have focused specifically on the statistical description of western boundary currents (Gulf Stream, Kuroshio) and particularly on their annual cycle (Fu *et al.*, 1987; Kelly and Gille, 1990; Tai, 1990; Tai and White, 1990; Vasquez *et al.*, 1990; Kelly, 1991; Qiu *et al.*, 1991; Zlotnicki, 1991).

Tai and White (1990) have done a detailed statistical analysis of one year of Geosat data in the Kuroshio extension to study the energy propagation away from the jet, the Reynolds stress pattern and the seasonal cycle of the eddy field (Fig. 13). Residual data of ascending tracks are first objectively analyzed assuming spatial decorrelation of 200 km and no time lag over each cycle (most of the descending tracks are gappy or missing in this area). Space-time diagrams and frequency-wave number spectra are then used to study the dominant direction of phase and energy propagation. The phase propagation appears to be toward the jet (assumed to be at 35°N). Using the dispersion relation of Rossby waves, Tai and White (1990) infer a group velocity away from the jet which could result from radiation of Rossby waves in response to meander forcing. Reynolds stresses show that the eddy flux of momentum is towards the jet and tends to strengthen it. On the north and south sides of the jet, the Reynolds stresses $\langle u'v' \rangle$ induce an eastward acceleration thus drive recirculation. This suggests baroclinic instability. All these results help to understand the eddy dynamics (energy source, energy propagation). However, the objective analysis method used which assumes isotropy (*i. e.*, zero Reynolds stresses $\langle u'v' \rangle$) probably conceals some of the dynamic features present in the data. The eddy field is found to have a seasonal cycle related to seasonal variation in surface transport. These signals are the weakest in winter and become progressively stronger towards the fall.

Vasquez *et al.* (1990) have examined more than two years of Geosat data in the Gulf Stream. Using ascending tracks only, they have mapped the sea level variability every ten days using a successive correction scheme. They have calculated mean temporal spectra at four locations along the Gulf Stream path (72°W, 65°W, 60°W and 55°W). Spectra slopes are between - 1.5 and - 0.9. Spectra tend to be whiter eastward because of the greater high-frequency energy, a result consistent with the Eulerian time scales obtained by Kelly (1991) and Le Traon (1991; *see* Fig. 11). The annual cycle accounts for 13 to 40 % of the total signal from east to west. Using a simple model based on AVHHR data, Vasquez *et al.* have also shown that this annual cycle can be largely explained by the meandering of a Gulf Stream with constant surface transport.

Kelly and Gille (1990) have studied the Gulf Stream statistics from Geosat at 69°W. The originality of their method is that they use a Gaussian velocity profile for the Gulf Stream to model sea surface height. From the comparison between model and data, they can infer the along-track width and its position. Theoretically, the model provides an estimate of the absolute signal provided there is enough displacement of the Gulf Stream axis over the time period. Kelly and Gille found that the annual transport cycle in the Gulf Stream reached a minimum in May-June and a maximum in November. This contrasted with previous altimetric studies (Fu *et al.*, 1987) and other estimates (*e. g.*, Worthington, 1976). The same result was found by Vasquez *et al.* (1990) and Tai and White (1990). Maximum and minimum transport of the Gulf Stream occur when the Gulf Stream is north and south respectively of its mean position. This study has been extended to the entire Gulf Stream by Kelly (1991), who described the Gulf Stream meandering and structure. Figure 14 shows the statistics for the mean positions of the Gulf Stream which were deduced from this study. Two different flow regimes, separated by a transition region coinciding with the New England Seamount Chain, are found west of 64°W and east of 58°W. East of 58°W, increased meandering makes the mean current twice as wide as west of 64°W. Eulerian time scales also drop by a factor of 3 and peak velocities and surface transport drop by 25 %. The single jet Gaussian model surprisingly accounts for most of the velocity variance in Geosat data, suggesting that it is an efficient description of the Gulf Stream structural changes. It is found again that more transport occurs at more northerly positions with the transport maximum leading the position maximum by about one month. Tai (1990) has used a similar method on an ensemble of ascending tracks in the Gulf Stream and Kuroshio extension. Surface transport is found to increase from 90 10^3 m^2s^{-2} (after leaving the coast) to reach a maximum of 130 10^3 m^2s^{-2} at 63°W for the Gulf Stream and at 150°E for the Kuroshio. These results compare well with surface transport deduced from drifter data (Richardson, 1985). The variability maximum coincides with the mean position of the jet.

Recently, Qiu *et al.* (1991) have refined the Kelly and Gille (1990) method. They estimate the two-dimensional mean surface height by combining synthetic profiles along ascending and descending tracks through an inverse method. Their method also accommodates possible modifications of the Gaussian shape such as possible recirculation gyres. This method was applied to 2.5 years of Geosat data in the Kuroshio. The mean sea surface height agrees well with the climatological mean obtained from hydrographic data. The ratio of eddy kinetic energy to mean kinetic energy has a nearly constant value of 1.5 to 2.0 along the Kuroshio path. Propagation of mesoscale fluctuations is generally westward except for the upstream region of the Kuroshio extension. Annual variations are found to be significant in the upstream region (141° to 153°E). On average, they explain only 15 % of the total variance while interannual variations explain 23 %. During the first two years of the Geosat Exact Repeat Mission (ERM) the Kuroshio extension as a whole shifted steadily northward at 0.1 km per day, while the surface height difference increased. This trend reversed during the following six months. Qiu *et al.* (1991) suggest that the increase in surface height difference may have been caused by the intensification of the subtropical wind gyre with the 1986-1987 ENSO event.

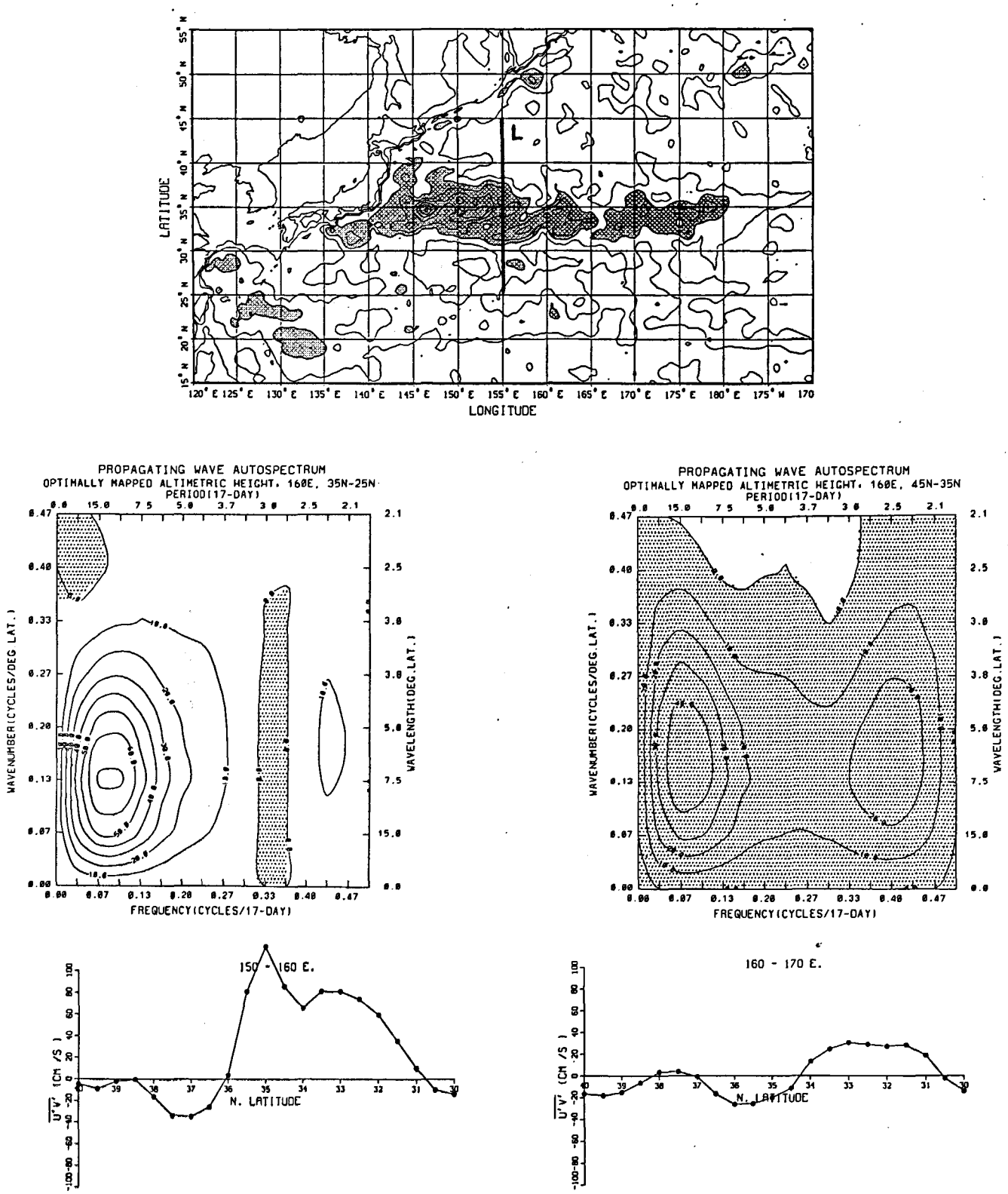

Figure 13

Statistical analysis of Geosat data in the Kuroshio extension. Rms sea level variability is shown on upper figure (values higher than 15 cm rms are shaded and contour interval is 5 cm). Propagating frequency-wave number spectra along the line L from 25°N to 35°N (left) and 35°N to 45°N (right; shading corresponds to southward propagation; middle figure). The phase propagation appears to be towards the jet (assumed to be at 35°N). Reynolds stresses <u'v'> in cm^2s^{-2} averaged zonally over 10° longitude and temporally over one year (bottom figure). The eddy flux of momentum is toward the jet and tends to reinforce the jet. North and south of the jet, the Reynolds stresses induce an eastward acceleration thus drive recirculation (reprinted by permission of American Meteorological Society).

Analyse statistique des données de Geosat au niveau du Kuroshio. L'écart-type de la variabilité du niveau de la mer est montré sur la figure du haut (les valeurs supérieures à 15 cm sont grisées, et l'intervalle de contour est de 5 cm). Spectres de propagation en fréquence et en nombre d'ondes le long de la ligne L de 25° à 35° N (à gauche) et de 35° à 45° N (à droite). Les zones grisées correspondent à des propagations vers le Sud (figures du milieu). La vitesse de phase est vers le jet (supposé situé à 35° N). Tensions de Reynolds en cm^2-s^{-2} moyennées zonalement sur 10° de longitude et temporellement sur une année (figure du bas). Le flux de quantité de mouvement est vers le jet et le renforce. Au nord et au sud du jet, les tensions de Reynolds impliquent une accélération vers l'est, et induisent donc une recirculation (reproduit avec la permission de l'Americain Meteorological Society).

Figure 14

Statistics on the position of the Gulf Stream derived from Geosat data [Kelly, 1991 (copyright by the American Geophysical Union)].

Statistiques sur la position du Gulf Stream obtenues à partir des données de Geosat [d'après Kelly, 1991 (copyright par l'American Geophysical Union)].

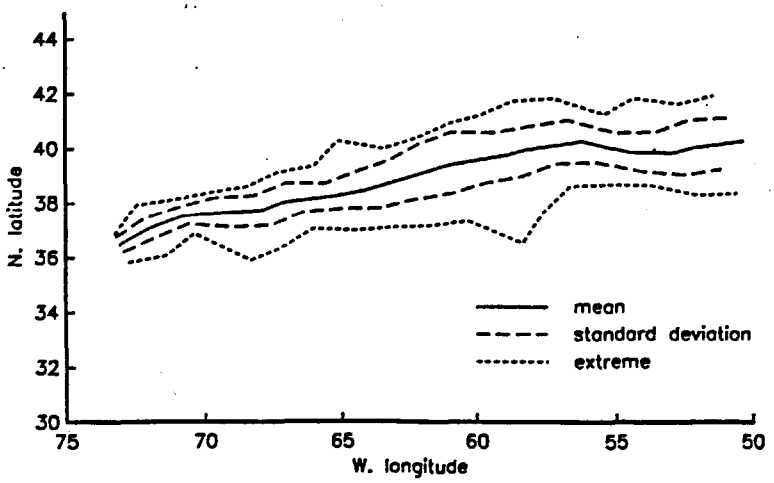

Zlotnicki's approach (1991) has been to estimate the sea level differences across the Gulf Stream and the Kuroshio extension. The south minus north differences (over approximately 10° of latitude) in both regions are higher in the fall. Some 60 % of this signal variance corresponds to an annual cycle with a maximum in late September-mid-October (9 cm for the Gulf Stream, 6.9 cm for the Kuroshio). These results also disagree with Fu *et al.* (1987) who found a maximum of 6 cm in April and a minimum of 8 cm in December. Zlotnicki argues that the signal seen by Fu *et al.* (1987) may reflect a change in the position of the Gulf Stream rather than a change in surface transport. Worthington (1976) has found that total transport of the Gulf Stream is higher in January through March (90 Sv) and lower in October through November (65-70 Sv). Kawabe (1988) has also found from tide gauge data a minimum transport in September-October in the Kuroshio. All these results diverge considerably from the Geosat results.

To conclude, it is fair to say that there is still work to do to rationalize the annual cycle of these western boundary currents. Note, however, that these studies have used at most two years of data which is too short a period to draw conclusions on these annual cycles. This short period may also explain differences between Geosat, GEOS-3 and *in situ* data. The synthetic methods used for some of the above studies are also really interesting since they can be used to estimate the absolute signal without knowing the geoid. They can be applied when lateral excursions of a current are comparable to or larger than the current's width. Prior knowledge of the current's functional form is also required. These results are also important for altimeter data assimilation. They show that, in certain conditions, altimetric residuals do contain information on the mean current and that the assimilation of residuals should provide control over part of the mean oceanic circulation.

CONCLUSION

We have attempted to describe the contribution that satellite altimetry has made to observing mesoscale ocean circulation. The study is based essentially on the data returned by the US Navy's Geosat altimeter which, by its long duration (nearly three years in a repeat orbit) and low noise level (about 3.5 cm rms) provided a quantitative description of the mesoscale circulation. The impressive number of referred publications concerning the analysis of Geosat data - over 100 from 1986 through 1991, of which about one third discussed mesoscale ocean circulation - is in itself very telling. We hope that our review of the results will be convincing enough to demonstrate the innovative contribution of Geosat data.

We began by summarizing the methods for recovering the mesoscale signal and discussing the measurement errors. We show that data processing and errors generally affect measurements of the ocean mesoscale signal only slightly, contamination being greater at longer spatial and temporal scales. This is confirmed by all the studies which have attempted to compare Geosat data with *in situ* data. Although the signals seen by the altimetry and the *in situ* instruments are generally different, as are the sampling modes, such studies have clearly shown Geosat's capabilities for observing mesoscale circulation even in low eddy energy areas.

The unique contribution of altimetry is its space-time coverage which can provide both a quasi-synoptic description and a statistical description of ocean surface circulation. Our examples show the exciting potential of synoptic mapping. One of the most representative studies is undoubtedly Gordon and Haxby (1990), which revealed the transport of 10 to 15 Sv of water from the Indian Ocean to the South Atlantic by eddies shed from the Agulhas retroflection. However, the greatest contribution is the statistical description of ocean mesoscale variability. Quantitative estimates of eddy energy have been obtained globally and have revealed previously unknown spatial details. Seasonal variations in eddy energy have also been estimated globally for the first time. One of the features revealed by studying these seasonal variations has been the possible role of forcing by fluctuating winds in certain parts of the ocean. The frequency/wave number mesoscale circulation spectrum has been characterized, as have the corresponding time and space scales. Eddy statistics have been visualized in greater detail, often bringing new information. Western boundary currents, in particular the Gulf Stream and Kuroshio, have

been studied very closely, revealing the complexity of the signals in these areas. Such studies are really useful to rationalize the structure of eddies and to understand eddy dynamics better. They are also a means of testing and validating models and theories. As models become more realistic in terms of resolution, bathymetry and wind forcing, their mesoscale features should thus be compared with these extensive statistical descriptions.

These results are also important for altimeter data assimilation. They clearly demonstrate Geosat's capabilities for observing and monitoring the instantaneous ocean eddy field even in low eddy energy areas. It shows that Geosat data can actually be assimilated into numerical oceanic models to infer the ocean three-dimensional circulation and its dynamics. Synthetic methods have also shown that, in certain conditions, altimetric residuals do contain information on the mean current, so that the assimilation of residuals should allow control over part of the mean oceanic circulation. Statistical descriptions of the oceanic mesoscale circulation obtained from Geosat data are also useful and often required for altimeter data assimilation studies.

There is still much to learn from Geosat data for mesoscale variability studies. First, detailed comparisons with models should help us to understand some of the Geosat results better. In particular, the frequency-wave number characteristics of altimeter sea level variability could be rationalized and possibly related to different kinds of forcing. The transfer function between the surface variability and the deeper mesoscale variability should also be investigated to estimate the relative importance of the mixed layer mesoscale variability (*e. g.,* Klein and Hua, 1988). This is important for the interpretation of altimeter data (*e. g.,* weak wave number spectral slopes) and for assimilation studies. Dedicated studies of relatively small regions could also be undertaken to describe their mesoscale characteristics in detail. In particular, most studies have dealt with high eddy energy areas. Relatively low eddy energy areas should now be investigated more systematically. For example, studies of eastern boundary dynamics could benefit a lot from satellite altimetry (*e. g.,* study of the generation and propagation of Rossby waves). The global mapping of Reynolds stresses (<u'v'>, <u'2>,<v'2>) at crossovers should also be very valuable for characterizing the eddy momentum fluxes and the anisotropy (although the inclination of Topex/Poseidon will be more suitable for these calculations). Despite the welcome contribution of Geosat, ERS-1 and Topex-Poseidon are expected to permit considerable further progress on mesoscale variability. First, the measurements will be more accurate, especially those by Topex-Poseidon. Second, dedicated experiments to calibrate and validate the altimeter data will provide accurate estimates of the errors induced on the ocean signal. More detailed studies and quantitative studies on low eddy energy will be possible. The largest spatial and temporal scales will also be available, and we will be able to study how they interact with mesoscale variability. Very substantial progress can be expected when ERS-1 (35-day orbit) data is combined with Topex-Poseidon data for synoptic mapping of ocean eddies. Comparing and combining the results with *in situ* data will also be instructive. For example, the comparison/combination of altimeter data with TOGA and WOCE surface drifter data should provide a means of estimating the ageostrophic component of the surface circulation, presently poorly known.

Finally, it may be noted that the assimilation of altimeter data in ocean models also contributes to a better understanding of mesoscale variability, and will make an ever greater contribution in the future. Dynamic interpolation of the data overcomes the shortcomings of altimeter sampling, and can provide the vertical structure of the mesoscale circulation from surface measurements. The work described in this special issue convincingly demonstrates the further significant contribution which altimetry can make to studies of mesoscale variability. It is the author's opinion, however, that there is still much to learn from the data themselves before assimilating them into numerical models.

REFERENCES

Bisagni J.J. (1989). Wet tropospheric range corrections for satellite altimeter-derived dynamic topographies in the Western North Atlantic. *J. geophys. Res.*, **94**, 3247-3254.

Blanc F., P.-Y. Le Traon and S. Houry (1992). A new method to extract mesocale variability from altimetry (in prep.).

Chelton D.B., M.G. Schlax, D.L. Witter and J.G. Richman (1990). Geosat altimeter observations of the surface circulation of the southern ocean. *J. geophys. Res.*, **95**, 17,877-17,903.

Cheney R.E., B.C. Douglas, R.W. Agreen, L. Miller, D. Milbert and D. Porter (1986). The Geosat altimeter mission: a milestone in satellite oceanography. *Eos*, **67**, 1354-1355.

De Mey P. (1992). Synoptic estimates of an eddy field in the North Atlantic Current. *Oceanologica Acta*, **15**, 5, 537-543 (this issue).

De Mey P. and Y. Ménard (1989). Synoptic analysis and dynamical adjustment of Geos3 and Seasat altimeter eddy fields in the North West Atlantic. *J. geophys. Res.*, **94**, 6221-6230.

Douglas B.C. and R.E. Cheney (1990). Geosat: beginning a new era in satellite oceanography. *J. geophys. Res.*, **95**, 2833-2836.

Eymard L. *et al.* (1991). The Semaphore mesoscale air-sea experiment (1993). Technical Report, Centre de Recherche sur la Physique de l'Environnement, Issy-les-Moulineaux, France.

Frankignoul C. and P. Müller (1979). Quasi-geostrophic response of an infinite b-plane ocean to stochastic forcing by the atmosphere. *J. phys. Oceanogr.*, **9**, 104-127.

Fu L.L. (1983 *a*). Recent progress in the application of satellite altimetry to observing the mesoscale variability and general circulation of the oceans. *Revs Geophys. Space Phys.*, **21**, 1657-1666.

Fu L.L. (1983 *b*). On the wave number spectrum of oceanic mesoscale variability observed by the Seasat altimeter. *J. geophys. Res.*, **88**, 4331-4341.

Fu L.L. and V. Zlotnicki (1989). Observing oceanic mesoscale eddies from Geosat altimetry: preliminary results. *Geophys. Res. Letts*, **16**, 457-460.

Fu L.L., J. Vasquez and M.E. Parke (1987). Seasonal variability of the Gulf Stream from satellite altimetry. *J. geophys. Res.*, **92**, 749-754.

Fu L.L, V. Zlotnicki and D.B. Chelton (1988). Satellite altimetry - observing ocean variability from space. *Oceanography*, **1**, 4-11, 58.

Glenn S.M., D.L. Porter and A.R. Robinson (1991). A synthetic geoid validation of Geosat mesoscale dynamic topography in the Gulf Stream region. *J. geophys. Res.*, **96**, 7145-7166.

Gordon A.L. and W.F. Haxby (1990). Agulhas eddies invade the south Atlantic: evidence from Geosat altimeter and shipboard conductivity temperature-depth survey. *J. geophys. Res.*, **95**, 3117-3125.

Hallock Z.R., J.L. Mitchell and J.D. Thompson (1989). Sea-surface topographic variability near the New England seamounts: an intercomparison among *in situ* observations, numerical simulations, and Geosat altimeter from the regional energetics experiment. *J. geophys. Res.*, **94**, 8021-8028.

Holland W.R., P.E. Harrison and A.J. Semtner (1982). Eddy resolving numerical models of large scale ocean circulation, in : *Eddies in marine science*, A.R Robinson, editor. Springer-Verlag, Berlin, 609 pp.

Hua B.L. and D.B. Haidvogel (1986). Numerical simulations of the vertical structure of quasi-geostrophic turbulence, *J. atmos. Sci.*, **43**, 2923-2936.

Jourdan D., C. Boissier, A. Braun and J.-F. Minster (1990). Influence of wet tropospheric correction on mesoscale dynamic topography as derived from satellite altimetry. *J. geophys. Res.*, **95**, 17993-18004.

Joyce T.M., K.A. Kelly, D.M. Schubert and M.J. Caruso (1990). Shipboard and altimetric studies of rapid Gulf Stream variability between Cape Cod and Bermuda. *Deep-Sea Res.*, **37**, 897-910.

Kawabe M. (1988). Variability of Kuroshio velocity assessed from the sea level difference between Naze and Nishinoomote. *J. oceanogr. Soc. Japan*, **44**, 293-304.

Kelly K.A. (1991). The meandering Gulf Stream as seen by the Geosat Altimeter: surface transport, position, and velocity variance from 73° to 46°W. *J. geophys. Res.*, **96**, 16721-16738.

Kelly K.A. and S.T. Gille (1990). Gulf stream surface transport and statistics at 69° W from the Geosat altimeter. *J. geophys. Res.*, **95**, 3149-3161.

Klein P. and B.L. Hua (1988). Mesoscale heterogeneity of the wind driven mixed layer: influence of a quasi-geostrophic flow. *J. mar. Res.*, **46**, 495-525.

Koblinsky C. (1988). Geosat *versus* Seasat. *Eos*, **69**, 1026.

Le Traon P.-Y. (1991). Time scales of mesoscale variability and their relationship with spatial scales in the North Atlantic. *J. mar. Res.*, **49**, 467-492.

Le Traon P.-Y. and F. Hernandez (1992). Mapping the oceanic mesoscale variability: validation of satellite altimetry using surface drifters. *J. atmos. ocean. Technol.*, in press.

Le Traon P.-Y., M.-C. Rouquet and C. Boissier (1990.) Spatial scales of mesoscale variability in the North Atlantic as deduced from Geosat data. *J. geophys. Res.*, **95**, 20267-20285.

Le Traon P.-Y., C. Boissier and P. Gaspar (1991). Analysis of errors due to polynomial adjustments of altimeter profiles. *J. atmos. ocean. Technol.*, **8**, 385-396.

Ménard Y. (1983). Observation of eddy fields in the northwestern Atlantic and northwestern Pacific by Seasat altimeter data. *J. geophys. Res.*, **88**, 1853-1866.

Mitchell J.L., J.M. Dastugue, W.J. Teague and Z.R. Hallock (1990). The estimation of geoid profiles in the northwest Atlantic from simultaneous satellite altimetry and airborne expendable bathythermograph sections. *J. geophys. Res.*, **95**, 17965-17977.

Monaldo F. (1990). Path length variations caused by atmospheric water vapor and their effects on the measurement of mesoscale ocean circulation features by a radar altimeter. *J. geophys. Res.*, **95**, 2923-2932.

Müller P. and C. Frankignoul (1981). Direct atmospheric forcing of geostrophic eddies. *J. phys. Oceanogr.*, **11**, 287-308.

Pares-Sierra A., W.B. White and C.K. Tai (1992). On the mesoscale variability in the California current system: a model-satellite data intercomparaison. *J. phys. Oceanogr.*, submitted.

Park Y.H. (1990). Mise en évidence d'ondes planétaires semi-annuelles dans le sud de l'Océan Indien par altimétrie satellitaire. *C.r. Acad. Sci., Paris*, **310**, 2, 919-926.

Ponte R.M. (1992). The sea level response of a stratified ocean to barometric pressure forcing. *J. phys. Oceanogr.*, **22**, 109-113.

Qiu B., K.A. Kelly and T.M. Joyce (1991). Mean flow and variability in the Kuroshio extension from Geosat altimetry data. *J. geophys. Res.*, **96**, 18491-18507.

Rhines P.B. (1977). The dynamics of unsteady currents, in: *Marine Modelling. The Sea*, E.D. Goldberg, I.N. McCane, J.J O'Brien and J.H. Steele, editors. Wiley and sons, 6, 189-318.

Richardson P.L. (1985). Average velocity and transport of the Gulf Stream near 55°W. *J. mar. Res.*, **43**, 83-111.

Robinson A.R. (1982). *Eddies in marine science*, A.R Robinson, editor. Springer-Verlag, Berlin, 609 pp.

Sandwell D.T. and B. Zhang (1989). Global mesoscale variability from the Geosat Exact Repeat Mission. Correlation with ocean depth. *J. geophys Res.*, **94**, 17971-17984.

Shum C.K, R.A. Werner, D.T. Sandwell, B.H. Zhang, R.S. Nerem and B.D. Tapley (1990). Variations of global mesoscale eddy energy observed from Geosat. *J. geophys. Res.*, **95**, 17865-17876.

Stammer D. and C.W. Böning (1992). Mesoscale variability in the Atlantic Ocean from Geosat altimetry and Woce high resolution numerical modelling. *J. phys. Oceanogr.*, **22**, 732-752.

Stammer D., H.H. Hinrichsen and R.H. Käse (1991). Can meddies be detected by satellite altimetry? *J. geophys. Res.*, **96**, 7005-7014.

Tai C.K. (1988). Geosat crossover analysis in the tropical Pacific. 1: Constrained sinusoidal crossover adjustment. *J. geophys. Res.*, **93**, 10, 10621-10629.

Tai C.K. (1990). Estimating the surface transport of meandering oceanic jet streams from satellite altimetry: surface transport estimates for the Gulf Stream and Kuroshio Extension. *J. phys. Oceanogr.*, **20**, 860-879.

Tai C.K. and L.L. Fu (1986). On crossover adjustment in satellite altimetry and its oceanographic implications. *J. geophys. Res.*, **91**, 2549-2554.

Tai C.K. and W.B. White (1990). Eddy variability in the Kuroshio extension as revealed by Geosat altimetry: energy propagation away from the jet, Reynolds stress, and seasonal cycle. J. *phys. Oceanogr.*, **20**, 1761-1777.

Tréguier A.M. (1992). Kinetic energy analysis of an eddy resolving, primitive equation model of the North Atlantic. *J. geophys. Res.*, **97**, 687-701.

Tréguier A.M. and B.L. Hua (1987). Oceanic quasi-geostrophic turbulence forced by stochastic wind fluctuations. *J. phys. Oceanogr.*, **17**, 397-411.

Tréguier A.M. and J.C. Mc Williams (1990). Topographic influences on wind-driven, stratified flow in a b-plane channel: an idealized model for the Antarctic circumpolar current. *J. phys. Oceanogr.*, **20**, 321-343.

Vasquez J., V. Zlotnicki and L.L. Fu (1990). Sea-level variabilities in the Gulf Stream between Cape Hatteras and 50°W. A Geosat study. *J. geophys. Res.*, **95**, 17957-17964.

White W.B., C.K. Tai and J. DiMento (1990). Annual Rossby waves characteristics in the California current region from the Geosat Exact Repeat Mission. *J. phys. Oceanogr.*, **20**, 1297-1311.

Willebrand J., R.H. Käse, D. Stammer, H.H. Hinrichsen and W. Krauss (1990). Verification of Geosat sea surface topography in the Gulf Stream extension with surface drifting buoys and hydrographic measurements. *J. geophys. Res.*, **95**, 2007-3014.

Worthington L.V. (1976). *On the North Atlantic Circulation*. The Johns Hopkins Oceanographic Studies, 110 pp.

Wunsch C. (1981). Low frequency variability in the sea, in : *Evolution of physical oceanography*, B. Warren and C. Wunsch, editors. MIT Press, Cambridge, Massachusetts, 342-374.

Zlotnicki V. (1991). Sea-level differences across the Gulf Stream and Kuroshio extension. *J. phys. Oceanogr.*, **21**, 599-609.

Zlotnicki V., L.L. Fu and W. Patzert (1989). Seasonal variability in global sea level observed with Geosat altimetry. *J. geophys. Res.*, **94**, 17959-17969.